crystals

MDPI

Article

Infrared Optical Conductivity of Bulk Bi_2Te_2Se

Elena S. Zhukova [1,2,*], Hongbin Zhang [3], Victor P. Martovitskiy [4], Yurii G. Selivanov [4], Boris P. Gorshunov [1,2] and Martin Dressel [1,2,*]

1 Moscow Institute of Physics and Technology, National Research University, 141701 Dolgoprudny, Moscow Region, Russia; gorshunov.bp@mipt.ru
2 1. Physikalisches Institut, Universität Stuttgart, Pfaffenwaldring 57, 70569 Stuttgart, Germany
3 Institute of Materials Science, Technische Universität Darmstadt, Jovanka-Bontschits-Str. 2, 64287 Darmstadt, Germany; hzhang@tmm.tu-darmstadt.de
4 P. N. Lebedev Physical Institute of the RAS, 119991 Moscow, Russia; victormart@yandex.ru (V.P.M.); selivan@lebedev.ru (Y.G.S.)
* Correspondence: zhukova.es@mipt.ru (E.S.Z.); martin.dressel@pi1.physik.uni-stuttgart.de (M.D.)

Received: 8 June 2020; Accepted: 24 June 2020; Published: 28 June 2020

Abstract: Mid- and near-infrared measurements reveal that the optical conductivity of the three-dimensional topological insulator, Bi_2Te_2Se, is dominated by bulk carriers and shows a linear-in-frequency increase at 0.5 to 0.8 eV. This linearity might be interpreted as a signature of three-dimensional (bulk) Dirac bands; however, band-structure calculations show that transitions between bands with complex dispersion contribute instead to the inter-band optical conductivity at these frequencies and, hence, the observed linearity is accidental. These results warn against the oversimplified interpretations of optical-conductivity measurements in different Dirac materials.

Keywords: topological insulators; optical conductivity; Dirac materials

1. Introduction

Spin-orbit coupling often leads to the formation of linear bands in solids. Electrons in such bands (the Dirac electrons) manifest themselves in special ways in different experiments [1–5]. One of these manifestations is in their optical response: the contribution of a *d*-dimensional Dirac band to the inter-band optical conductivity, which is calculated to follow a simple power–law frequency dependence [6,7]:

$$\sigma(\omega) \propto \omega^{d-2}. \quad (1)$$

Such optical-conductivity behavior—unusual for conventional materials—has indeed been confirmed for (quasi)-2D electrons in graphene, graphite, and the line-node semimetal ZrSiS, where $\sigma(\omega) \approx const(\omega)$ was reported [8–10]. In turn, the 3D Dirac electrons in Dirac and Weyl semimetals, such as $ZrTe_5$, Cd_3As_2, and TaAs, provide the inter-band optical conductivity to be proportional to frequency, $\sigma(\omega) \propto \omega$ [11–13]. The linearity in $\sigma(\omega)$ over a broad frequency range in a 3D electron system is often considered as a "smoking gun" for Dirac physics. For example, Timusk et al. [14] suggested the presence of 3D Dirac fermions in a number of quasicrystals, based entirely on the observation of a linear $\sigma(\omega)$ in these materials.

Besides, enormous efforts have been made to investigate the symmetry-protected surface states of topological insulators [2,3]. However, the dominant physics of the bulk often obscures the surface properties and hence is generally considered as an obstacle for experiments targeting the surface states. Achieving dissipationless surface spin currents may be of primary importance for potential applications of topological insulators, nevertheless, investigations into bulk electronic properties are essential for understanding the complete picture of the topological-state formation [15].

Our experiments reveal that the bulk optical conductivity of Bi_2Te_2Se follows a linear frequency dependence in an appreciably broad spectral range. Based on band-structure calculations, we argue that this linearity is not due to transitions within (a) particular 3D linear band(s), but instead a result of contributions from the transitions between the bands with complex dispersion.

2. Materials and Methods

Bi_2Te_2Se bulk crystals were synthesized by a modified Bridgman method [16]. Highly purified (99.9999%) elemental starting materials (Bi, Te, and Se) (Chimmed, Moscow, Russia) were loaded in quartz ampules inside an inert-gas glove box in the stoichiometric ratio 2:2:1. The sealed evacuated ampules were kept at 850 °C for 24 hours with periodic stirring to ensure the homogeneity of the melt, followed by a cooldown to 520 °C with a rate of 5 °C/hour. The crystals were then annealed at 520 °C for six days. The typical crystal sizes obtained in this way were in the centimeter range. The crystals were cut into appropriate pieces for X-ray, Hall, and optical measurements (and kept in vacuum until the measurements).

Utilizing an X'Pert Pro Extended MRD X-ray diffractometer (PANalytical, Almelo, the Netherlands) we have confirmed the high structural quality of the crystals, see Figure 1. The free-carrier concentration and mobility were measured in a standard Hall geometry. Indium-soldered contacts were applied to razor-cut Hall bars with typical dimensions of $2 \times 0.5 \times 0.2$ mm^3. For all samples, the conduction was by *n*-type carriers. The properties of the sample, used in our infrared studies, are listed in Table 1.

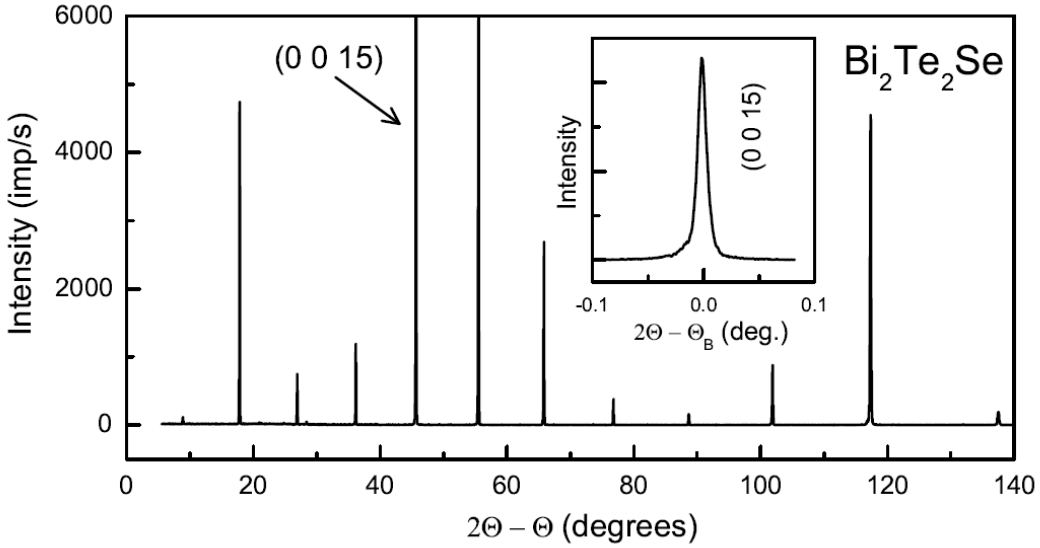

Figure 1. Bi_2Te_2Se X-ray diffraction pattern. Inset: Rocking curve for the (0 0 15) reflection peak.

Table 1. Room-temperature properties of the single-crystalline Bi_2Te_2Se sample used for the optical measurements. The mobility value is typical for the samples with such electron densities [17].

Lateral Dimensions	Thickness	Bulk electron Density	Mobility	Lattice Constant
5×5 mm^2	350 μm	1.0×10^{18} cm^{-3}	330 cm^2/Vs	29.766 A

Optical reflectivity was measured from the (001) plane on freshly cleaved surfaces. The room-temperature experiments were performed in the mid- and near-infrared spectral ranges (600–8000 cm^{-1}, 75 meV–1 eV) with a Bruker Vertex 80v Fourier-transform infrared spectrometer (Bruker Corporation, Billerica, MA, USA). Freshly evaporated gold mirrors served for reference measurements. We used unpolarized light, because Bi_2Te_2Se possesses C_3 rotational symmetry along the [001] direction and hence the (001)-plane response, expressed via a second-rank tensor, such as optical conductivity, is isotropic.

3. Results and Discussion

In the top panel of Figure 2, we plot the raw reflectivity data recorded at 300 K. The reflectivity is very flat between 4000 and 8000 cm^{-1}. In order to obtain the optical conductivity from the reflectivity data, we first tried to fit the measured spectra using a standard Drude–Lorentz procedure [18]. However, we found that such flat reflectivity is impossible to fit in an acceptable way with a physically meaningful number of Lorentzians. In an alternative approach, we used Kuzmenko's variational dielectric function method [19], which produces optical functions with an accuracy equivalent to Kramers–Kronig. For the sake of convenience, the variable part of the dielectric response function was described by a large number of Lorentzians. Justification and details of this approach can be found in [20]. Similar to the Kramers–Kronig analysis, this method gives less accurate results near the edges of the experimental window. Thus, the results below approximately 2000 cm^{-1} and above 7000 cm^{-1} cannot be considered as accurate.

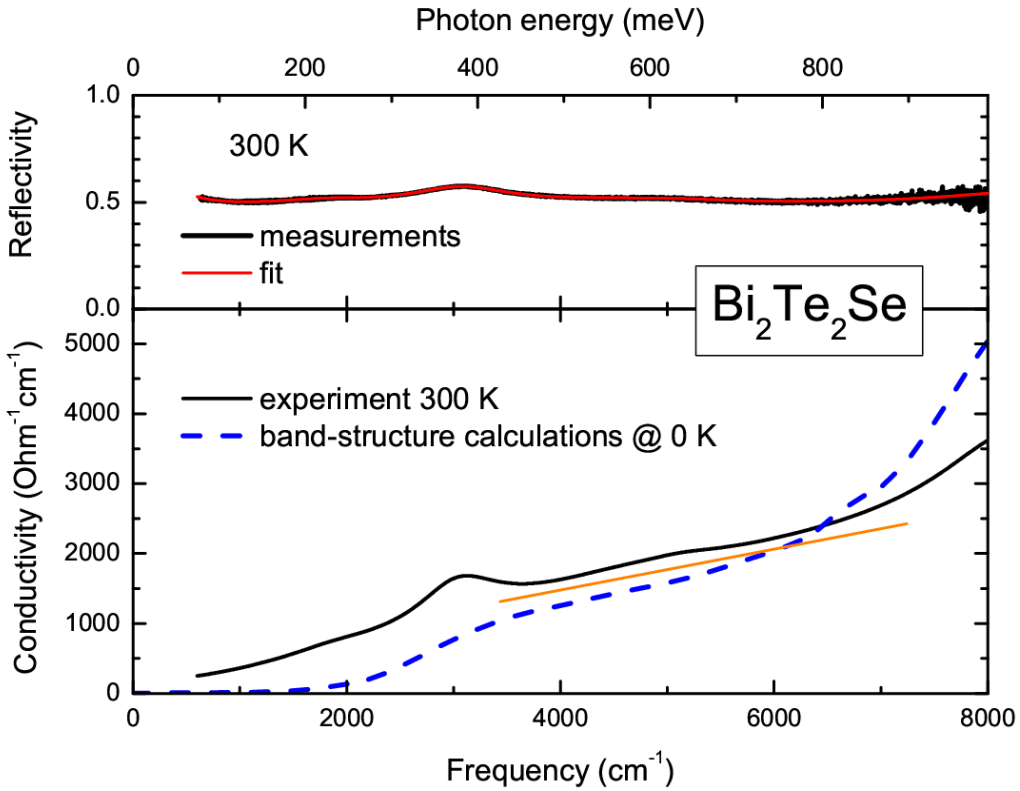

Figure 2. Top panel: [001]-plane reflectivity of Bi_2Te_2Se at 300 K: measurements (black line) and fit (red line). Bottom panel: bulk optical conductivity (real part) of Bi_2Te_2Se, as obtained from the reflectivity fit (black straight line) and the inter-band portion of optical conductivity, computed from the band structure of Figure 3 at 0 K (dashed line), as detailed in the text. The thin orange line is to mimic a linear increase in frequency.

The real part of the optical conductivity obtained from this fit is plotted in the bottom panel of Figure 2. The eye-catching feature of the figure is the linear increase in $\sigma(\omega)$ at 4000 to 7000 cm^{-1} (~0.5–0.8 eV).

Let us first argue that the observed optical conductivity originates from the bulk of Bi_2Te_2Se. In Bi_2Te_2Se, the surface Dirac point lies inside the bulk band gap [21,22] and metallic surface states have been experimentally confirmed [21–27]. Nevertheless, Bi_2Te_2Se samples usually possess a significant concentration of bulk charges due to the basically unavoidable presence of defects, the so-called self-doping [26–30]. This is also the case for our sample—its bulk carrier concentration is rather large, as shown in Table 1. Furthermore, the skin depth, calculated from the complex optical conductivity,

is above 30 nm at any measurement frequency, while the thickness of the topologically non-trivial surface layer is believed to be around 1 nm [3]. Hence, the response detected by our optical measurements is due to the bulk.

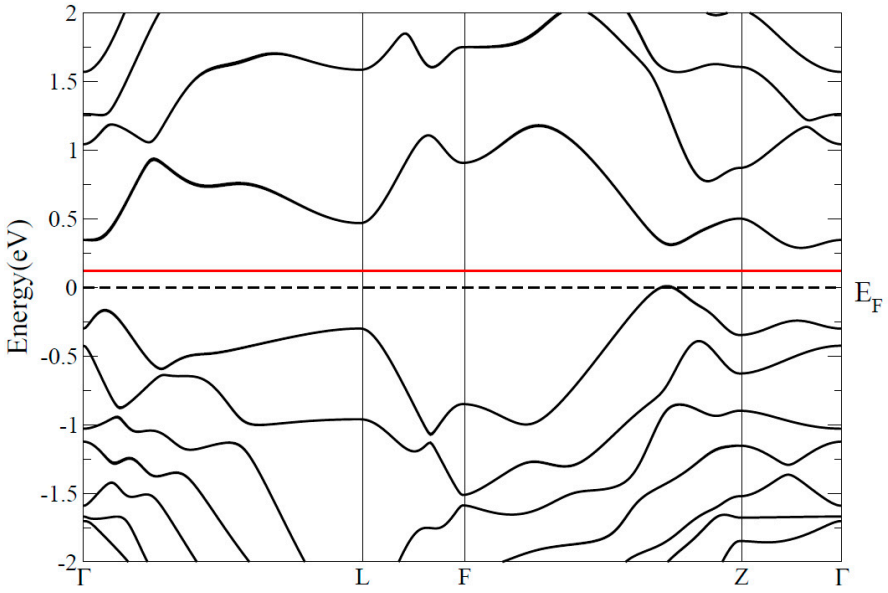

Figure 3. Band structure of Bi_2Te_2Se. Black dashed (red solid) horizontal line indicates the original (shifted) Fermi energy.

Let us also note that, at elevated temperatures, the optical detection of surface carriers in Bi_2Te_2Se, as well as in similar compounds, such as Bi_2Te_3 and Bi_2Se_3, remains so far elusive, while bulk carriers clearly manifest themselves in the optical response of Bi_2Te_2Se [16,28–30] and related compounds [31–35]. Reijnders et al. have reported on a mixed (surface plus bulk) optical response in Bi_2Te_2Se for low frequencies at temperatures below some 40 K [30]. However, at room temperature, as well as at frequencies above 2000 cm^{-1}, their data are perfectly reconciled with entirely bulk response.

Coming back to the linear $\sigma(\omega)$, it is tempting to interpret it in terms of Equation (1), namely, as a signature of a 3D Dirac band (because our $\sigma(\omega)$ reflects the bulk response). Such a band, however, is not expected to appear in the bulk of Bi_2Te_2Se [36]. We would like to point out that all the available optical conductivity spectra (ours and those previously reported in [16,28–30]) are rather similar to each other, although the linearity of $\sigma(\omega)$ is most apparent in our data. The deviations between the data sets can be assigned, for example, to the abovementioned difference in the exact Fermi-level position in different samples of Bi_2Te_2Se. In order to check the origin of the linear frequency increase in $\sigma(\omega)$, we performed band-structure calculations for Bi_2Te_2Se and then calculated its inter-band optical conductivity.

The band-structure and optical-conductivity calculations were performed using the full potential linear augmented plane-wave method, as implemented in the WIEN2k code [37]. The exchange-correlation functional is parameterized using the GGA approximation [38]. The self-consistent charge-densities and optical-conductivity calculations were done with 400 and 2000 k-points in the whole Brillouin zone, respectively. The results of the calculations are shown in Figures 2 and 3. The obtained band structure is basically identical to the one reported in [36]. In order to be reconciled with the bulk electron concentration (the self-doping problem mentioned above), the Fermi level needs to be shifted upwards, as compared to the undoped situation, as shown in Figure 3. From the figure, it is apparent that there is no truly Dirac band in the bulk of Bi_2Te_2Se.

The calculated optical conductivity is shown as a dashed line in Figure 2. Taking into account the generally poor reproducibility of the experimental infrared optical conductivity by first-principles

calculations (cf., e.g., in [39,40]), the agreement between theory and experiment can be considered as fairly good. Further, we should point out that the computed σ(ω) has no intra-band (free-carrier) contribution. Thus, it is not surprising that the low-frequency experimental σ(ω) is larger than the theoretical line. Additionally, the effect of temperature broadening is absent in the calculations. Such broadening would make the smooth step at around 3000 cm^{-1} even broader [10].Taking into account the mentioned issues in the computations of σ(ω) is outside of our capacity and beyond the scope of the paper. The important result of our computations is that the linear σ(ω) is nicely reproduced at 4000 to 6000 cm^{-1} (~0.5–0.75 eV). Thus, we can conclude that this linearity comes as a cumulative effect of transitions between the bands, which do not have a simple linear dispersion. We note that recent measurements of $BaCoS_2$ and GdPtBi provide other examples of linear σ(ω) not due to a simple 3D Dirac band [41,42].

4. Conclusions

We have experimentally found that the bulk optical conductivity of Bi_2Te_2Se is linear in frequency at 4000 to 7000 cm^{-1} (~0.5–0.8 eV). Our computations demonstrate that this linearity is not due to transitions within a 3D Dirac band, but emerges as a cumulative effect of transitions between the bands with complex dispersion. Obviously, similar situations can appear in other systems and, thus, suggestions for Dirac physics based on optical-conductivity measurements have to be made cautiously.

Author Contributions: Infrared measurements, E.S.Z. and B.P.G.; sample preparation, V.P.M. and Y.G.S.; data analysis, E.S.Z.; writing—original draft preparation, E.S.Z.; writing—review and editing, H.Z., M.D., and B.P.G.; project administration, B.P.G.; funding acquisition, Y.G.S. M.D., and B.P.G. All authors have read and agreed to the published version of the manuscript.

Funding: This work was supported by the Ministry of Science and Higher Education of the Russian Federation (Program "5 top 100"), by the Russian Science Foundation (grant No. 17-12-01544) and by the Deutsche Forschungsgemeinschaft (DFG) via grants No. DR228/51 and No. ZH559/2-1.

Conflicts of Interest: The authors declare no conflict of interest. The funders had no role in the design of the study; in the collection, analyses, or interpretation of data; in the writing of the manuscript, or in the decision to publish the results.

References

1. Neto, A.C.; Guinea, F.; Peres, N.; Novoselov, K.S.; Geim, A.K. The electronic properties of graphene. *Rev. Mod. Phys.* **2009**, *81*, 109. [CrossRef]
2. Hasan, M.Z.; Kane, C.L. Colloquium: Topological insulators. *Rev. Mod. Phys.* **2010**, *82*, 3045. [CrossRef]
3. Qi, X.L.; Zhang, S.C. Topological insulators and superconductors. *Rev. Mod. Phys.* **2011**, *83*, 1057. [CrossRef]
4. Wehling, T.O.; Black-Schaffer, A.M.; Balatsky, A.V. Dirac materials. *Adv. Phys.* **2014**, *63*, 1. [CrossRef]
5. Armitage, N.P.; Mele, E.J.; Vishwanath, A. Weyl and Dirac semimetals in three-dimensional solids. *Rev. Mod. Phys.* **2018**, *90*, 015001. [CrossRef]
6. Hosur, P.; Parameswaran, S.A.; Vishwanath, A. Charge transport in Weyl semimetals. *Phys. Rev. Lett.* **2012**, *108*, 046602. [CrossRef] [PubMed]
7. Bacsi, A.; Virosztek, A. Low-frequency optical conductivity in graphene and in other scale-invariant two-band systems. *Phys. Rev. B* **2013**, *87*, 125425. [CrossRef]
8. Kuzmenko, A.B.; van Heumen, E.; Carbone, F.; van der Marel, D. Universal Optical conductance of graphite. *Phys. Rev. Lett.* **2008**, *100*, 117401. [CrossRef]
9. Mak, K.F.; Sfeir, M.Y.; Wu, Y.; Lui, C.H.; Misewich, J.A.; Heinz, T.F. Measurement of the Optical conductivity of graphene. *Phys. Rev. Lett.* **2008**, *101*, 196405. [CrossRef]
10. Schilling, M.B.; Schoop, L.M.; Lotsch, B.V.; Dressel, M.; Pronin, A.V. Flat Optical Conductivity in ZrSiS due to two-dimensional Dirac bands. *Phys. Rev. Lett.* **2017**, *119*, 187401. [CrossRef]
11. Chen, R.Y.; Zhang, S.J.; Schneeloch, J.A.; Zhang, C.; Li, Q.; Gu, G.D.; Wang, N.L. Optical spectroscopy study of the three-dimensional Dirac semimetal $ZrTe_5$. *Phys. Rev. B* **2015**, *92*, 075107. [CrossRef]
12. Neubauer, D.; Carbotte, J.P.; Nateprov, A.A.; Löhle, A.; Dressel, M.; Pronin, A.V. Interband optical conductivity of the [001]-oriented Dirac semimetal Cd_3As_2. *Phys. Rev. B* **2016**, *93*, 121202. [CrossRef]

13. Xu, B.; Dai, Y.M.; Zhao, L.X.; Wang, K.; Yang, R.; Zhang, W.; Liu, J.Y.; Xiao, H.; Chen, G.F.; Taylor, A.J.; et al. Optical spectroscopy of the Weyl semimetal TaAs. *Phys. Rev. B* **2016**, *93*, 121110. [CrossRef]
14. Timusk, T.; Carbotte, J.P.; Homes, C.C.; Basov, D.N.; Sharapov, S.G. Three-dimensional Dirac fermions in quasicrystals as seen via optical conductivity. *Phys. Rev. B* **2013**, *87*, 235121. [CrossRef]
15. Xu, S.-Y.; Xia, Y.; Wray, L.A.; Jia, S.; Meier, F.; Dil, J.H.; Osterwalder, J.; Slomski, B.; Bansil, A.; Lin, H.; et al. Topological phase transition and texture inversion in a tunable topological insulator. *Science* **2011**, *332*, 560. [CrossRef]
16. Aleshchenko, Y.A.; Muratov, A.V.; Pavlova, V.V.; Selivanov, Y.G.; Chizhevskii, E.G. Infrared spectroscopy of Bi_2Te_2Se. *JETP Lett.* **2014**, *99*, 187. [CrossRef]
17. Jia, S.; Ji, H.; Climent-Pascual, E.; Fuccillo, M.K.; Charles, M.E.; Xiong, J.; Ong, N.P.; Cava, R.J. Low-carrier-concentration crystals of the topological insulator Bi_2Te_2Se. *Phys. Rev. B* **2011**, *84*, 235206. [CrossRef]
18. Dressel, M.; Grüner, G. *Electrodynamics of Solids*; Cambridge University Press: Cambridge, UK, 2002.
19. Kuzmenko, A.B. Kramers–Kronig constrained variational analysis of optical spectra. *Rev. Sci. Instrum.* **2005**, *76*, 083108. [CrossRef]
20. Chanda, G.; Lobo, R.P.S.M.; Schachinger, E.; Wosnitza, J.; Naito, M.; Pronin, A.V. Optical study of superconducting Pr_2CuO_x with x≃4. *Phys. Rev. B* **2014**, *90*, 024503. [CrossRef]
21. Xu, S.-Y.; Wray, L.A.; Xia, Y.; Shankar, R.; Petersen, A.; Fedorov, A.; Lin, H.; Bansil, A.; Hor, Y.S.; Grauer, D.; et al. Discovery of several large families of topological insulator classes with backscattering-suppressed spin-polarized single-Dirac-cone on the surface. *arXiv* **2010**, arXiv:1007.5111.
22. Ren, Z.; Taskin, A.A.; Sasaki, S.; Segawa, K.; Ando, Y. Large bulk resistivity and surface quantum oscillations in the topological insulator Bi_2Te_2Se. *Phys. Rev. B* **2010**, *82*, 241306. [CrossRef]
23. Xiong, J.; Petersen, A.C.; Qu, D.; Hor, Y.S.; Cava, R.J.; Ong, N.P. Quantum oscillations in a topological insulator Bi_2Te_2Se with large bulk resistivity (6 Ωcm). *Physica E* **2012**, *44*, 917. [CrossRef]
24. Li, Z.; Chen, T.; Pan, H.; Song, F.; Wang, B.; Han, J.; Qin, Y.; Wang, X.; Zhang, R.; Wan, J.; et al. Two-dimensional universal conductance fluctuations and the electron-phonon interaction of surface states in Bi_2Te_2Se microflakes. *Sci. Rep.* **2012**, *2*, 595. [CrossRef] [PubMed]
25. Tian, J.; Miotkowski, I.; Hong, S.; Chen, Y.P. Electrical injection and detection of spin-polarized currents in topological insulator Bi_2Te_2Se. *Sci. Rep.* **2015**, *5*, 14293. [CrossRef]
26. Arakane, T.; Sato, T.; Souma, S.; Kosaka, K.; Nakayama, K.; Komatsu, M.; Takahashi, T.; Ren, Z.; Segawa, K.; Ando, Y. Tunable Dirac cone in the topological insulator $Bi_{2-x}Sb_xTe_{3-y}Se_y$. *Nat. Commun.* **2011**, *3*, 636. [CrossRef]
27. Neupane, M.; Xu, S.-Y.; Wray, L.A.; Petersen, A.; Shankar, R.; Alidoust, N.; Liu, C.; Fedorov, A.; Ji, H.; Allred, J.M.; et al. Topological surface states and Dirac point tuning in ternary topological insulators. *Phys. Rev. B* **2012**, *85*, 235406. [CrossRef]
28. di Pietro, P.; Vitucci, F.M.; Nicoletti, D.; Baldassarre, L.; Calvani, P.; Cava, R.; Hor, Y.S.; Schade, U.; Lupi, S. Ab initio studying of topological insulator Bi_2Se_3 under the stress. *Phys. Rev. B* **2012**, *86*, 045439. [CrossRef]
29. Akrap, A.; Tran, M.; Ubaldini, A.; Teyssier, J.; Giannini, E.; van der Marel, D.; Lerch, P.; Homes, C.C. Optical properties of Bi_2Te_2Se at ambient and high pressures. *Phys. Rev. B* **2012**, *86*, 235207. [CrossRef]
30. Reijnders, A.A.; Tian, Y.; Sandilands, L.J.; Pohl, G.; Kivlichan, I.D.; Zhao, S.Y.F.; Jia, S.; Charles, M.E.; Cava, R.J.; Alidoust, N.; et al. Optical evidence of surface state suppression in Bi-based topological insulators. *Phys. Rev. B* **2014**, *89*, 075138. [CrossRef]
31. LaForge, A.D.; Frenzel, A.; Pursley, B.C.; Lin, T.; Liu, X.; Shi, J.; Basov, D.N. Optical characterization of Bi_2Se_3 in a magnetic field: Infrared evidence for magnetoelectric coupling in a topological insulator material. *Phys. Rev. B* **2010**, *81*, 125120. [CrossRef]
32. Sushkov, A.B.; Jenkins, G.S.; Schmadel, D.C.; Butch, N.P.; Paglione, J.; Drew, H.D. Far-infrared cyclotron resonance and Faraday effect in Bi_2Se_3. *Phys. Rev. B* **2010**, *82*, 125110. [CrossRef]
33. Dordevic, S.V.; Wolf, M.S.; Stojilovic, N.; Lei, H.; Petrovic, C. Signatures of charge inhomogeneities in the infrared spectra of topological insulators Bi_2Se_3, Bi_2Te_3 and Sb_2Te_3. *J. Phys. Condens. Matter* **2013**, *25*, 075501. [CrossRef] [PubMed]
34. Chapler, B.C.; Post, K.W.; Richardella, A.R.; Lee, J.S.; Tao, J.; Samarth, N.; Basov, D.N. Infrared electrodynamics and ferromagnetism in the topological semiconductors Bi_2Te_3 and Mn-doped Bi_2Te_3. *Phys. Rev. B* **2014**, *89*, 235308. [CrossRef]

35. Post, K.W.; Lee, Y.S.; Chapler, B.C.; Schafgans, A.A.; Novak, M.; Taskin, A.A.; Segawa, K.; Goldflam, M.D.; Stinson, H.T.; Ando, Y.; et al. Infrared probe of the bulk insulating response in $Bi_{2-x}Sb_xTe_{3-y}Se_y$ topological insulator alloys. *Phys. Rev. B* **2015**, *91*, 165202. [CrossRef]
36. Wang, L.-L.; Johnson, D.D. Ternary tetradymite compounds as topological insulators. *Phys. Rev. B* **2011**, *83*, 241309. [CrossRef]
37. Available online: http://www.wien2k.at (accessed on 6 June 2020).
38. Perdew, J.P.; Burke, K.; Ernzerhof, M. Generalized gradient approximation made simple. *Phys. Rev. Lett.* **1996**, *77*, 3865. [CrossRef]
39. Frenzel, A.J.; Homes, C.C.; Gibson, Q.D.; Shao, Y.M.; Post, K.W.; Charnukha, A.; Cava, R.J.; Basov, D.N. Anisotropic electrodynamics of type-II Weyl semimetal candidate WTe_2. *Phys. Rev. B* **2017**, *95*, 245140. [CrossRef]
40. Neubauer, D.; Yaresko, A.; Li, W.; Löhle, A.; Hübner, R.; Schilling, M.B.; Shekhar, C.; Felser, C.; Dressel, M.; Pronin, A.V. Optical conductivity of the Weyl semimetal NbP. *Phys. Rev. B* **2018**, *98*, 195203. [CrossRef]
41. Santos-Cottin, D.; Klein, Y.; Werner, P.; Miyake, T.; Medici, L.d.; Gauzzi, A.; Lobo, R.P.S.M.; Casula, M. Linear behavior of the optical conductivity and incoherent charge transport in $BaCoS_2$. *Phys. Rev. Materials* **2018**, *2*, 105001. [CrossRef]
42. Hütt, F.; Yaresko, A.; Schilling, M.B.; Shekhar, C.; Felser, C.; Dressel, M.; Pronin, A.V. Linear-in-frequency optical conductivity in GdPtBi due to transitions near the triple points. *Phys. Rev. Lett.* **2018**, *121*, 176601. [CrossRef]